


**ORIGINAL RESEARCH**

---

# Microbe-Derived Butyrate and Its Receptor, Free Fatty Acid Receptor 3, But Not Free Fatty Acid Receptor 2, Mitigate Neointimal Hyperplasia Susceptibility After Arterial Injury

Michael Nooromid, MD\*; Edmund B. Chen, MD\*; Liqun Xiong, BS; Katherine Shapiro, BA; Qun Jiang, MD; Falen Demsas, BS, MA; Maeve Eskandari; Medha Priyadarshini, PhD; Eugene B. Chang, MD; Brian T. Layden, MD, PhD; Karen J. Ho , MD

**BACKGROUND:** Arterial restenosis after vascular surgery is a common cause of midterm restenosis and treatment failure. Herein, we aim to investigate the role of microbe-derived butyrate, FFAR2 (free fatty acid receptor 2), and FFAR3 (free fatty acid receptor 3) in mitigating neointimal hyperplasia development in remodeling murine arteries after injury.

**METHODS AND RESULTS:** C57BL/6 mice treated with oral vancomycin before unilateral femoral wire injury to deplete gut microbiota had significantly diminished serum and stool butyrate and more neointimal hyperplasia development after arterial injury, which was reversed by concomitant butyrate supplementation. Deficiency of FFAR3 but not FFAR2, both receptors for butyrate, exacerbated neointimal hyperplasia development after injury. FFAR3 deficiency was also associated with delayed recovery of the endothelial layer in vivo. FFAR3 gene expression was observed in multiple peripheral arteries, and expression was increased after arterial injury. Treatment of endothelial but not vascular smooth muscle cells with the pharmacologic FFAR3 agonist 1-methylcyclopropane carboxylate stimulated cellular migration and proliferation in scratch assays.

**CONCLUSIONS:** Our results support a protective role for butyrate and FFAR3 in the development of neointimal hyperplasia after arterial injury and delineate activation of the butyrate-FFAR3 pathway as a valuable strategy for the prevention and treatment of neointimal hyperplasia.

**Key Words:** butyrate ■ neointimal hyperplasia ■ restenosis

---

Each year in the United States, 7.4 million patients with cardiovascular disease undergo revascularization procedures, such as balloon angioplasty, stenting, and surgical bypass.<sup>1</sup> However, despite decades of advancements in high-intensity statin therapy,<sup>2–5</sup> antiplatelet therapy,<sup>6,7</sup> drug-coated balloons, and drug-eluting stents,<sup>8,9</sup> up to 50% of treated

vessels will exhibit recurrent narrowing, or restenosis, within 1 year because of the formation of neointimal hyperplasia, a pathologic response of the blood vessel to the procedure that is distinct from progression of atherosclerosis.<sup>9</sup> Neointimal hyperplasia is a local inflammatory and proliferative process initiated by endothelial denudation. Although both genetic and

---

Correspondence to: Karen J. Ho, MD, Department of Surgery, Feinberg School of Medicine, Northwestern University, 676 N St Clair St, Suite 650, Chicago, IL 60611. E-mail: kho1@nm.org

\*Dr Nooromid and Dr Chen contributed equally to this work.

For Sources of Funding and Disclosures, see page 10.

© 2020 The Authors. Published on behalf of the American Heart Association, Inc., by Wiley. This is an open access article under the terms of the Creative Commons Attribution-NonCommercial-NoDerivs License, which permits use and distribution in any medium, provided the original work is properly cited, the use is non-commercial and no modifications or adaptations are made.

JAHA is available at: [www.ahajournals.org/journal/jaha](http://www.ahajournals.org/journal/jaha)

## CLINICAL PERSPECTIVE

### What Is New?

- Although reports of the role of gut microbiota in cardiovascular diseases, such as atherosclerosis and hypertension, are becoming increasingly abundant, the link between dysbiosis and neointimal hyperplasia development as a cause of arterial restenosis after arterial injury and vascular surgery is less clear.
- We observed that microbe-derived butyrate and its receptor, FFAR3 (free fatty acid receptor 3), but not FFAR2 (free fatty acid receptor 2), have a mitigating effect on the development of neointimal hyperplasia in a murine model of arterial injury and that pharmacologic FFAR3 agonism stimulates endothelial proliferation and migration

### What Are the Clinical Implications?

- These findings suggest a mechanistic link between microbial production of butyrate and host FFAR3 expression and activity in remodeling peripheral arteries, highlighting a potentially important role of the microbe-host interaction in the arterial remodeling response after cardiovascular surgery

## Nonstandard Abbreviations and Acronyms

<b>1-MCPC</b>	1-methylcyclopropane carboxylate
<b>EC</b>	endothelial cell
<b>FFAR2</b>	free fatty acid receptor 2
<b>FFAR3</b>	free fatty acid receptor 3
<b>GPCR</b>	G-protein–coupled receptor
<b>SCFA</b>	short-chain fatty acid
<b>VSMC</b>	vascular smooth muscle cell
<b>WT</b>	wild type

environmental factors contribute, the precise nature of gene-environment interactions underlying pathologic intima formation after surgery remains obscure.

A growing body of literature supports a direct role for microbiota in cardiovascular disease pathologic features through bioactive microbe-derived chemicals.<sup>10</sup> In humans, patients with symptomatic atherosclerosis have depleted abundance of butyrate-producing microbes *Eubacterium* and *Roseburia* compared with controls.<sup>11</sup> The microbiomes of patients with coronary artery disease have also been found to have depletion of butyrate-producing Lachnospiraceae and Ruminococcaceae compared with patients without coronary artery disease.<sup>12</sup> However, the role of

microbe-derived butyrate in the arterial remodeling response after surgery is not well known. We previously demonstrated that antibiotic-treated rats had exacerbated neointimal hyperplasia development after carotid angioplasty, which was associated with diminished butyrate. Butyrate was also found to inhibit vascular smooth muscle cell (VSMC) migration, proliferation, and cell cycle progression in vitro, implicating a beneficial role for butyrate in the arterial remodeling response after surgery.<sup>13</sup>

Butyrate is a principal short-chain fatty acid (SCFA) produced in millimolar amounts in the colonic lumen by microbiota.<sup>14</sup> SCFAs exert their physiological effects in part by activating nutrient-sensing free fatty acid GPCRs (G-protein–coupled receptors), such as FFAR2 (free fatty acid receptor 2; also known as GPR43, or FFA2) and FFAR3 (free fatty acid receptor 3; also known as GPR41 or FFA3).<sup>15</sup> Butyrate is passively absorbed from the intestinal lumen and is oxidized by colonic epithelial cells as an energy source. Unused butyrate is taken up into the portal circulation and released into the plasma.<sup>14,16</sup> The goal of this study is to understand the role of FFAR2 and FFAR3 in mediating the effects of butyrate on neointimal hyperplasia using a mouse model of arterial injury.

## METHODS

The data that support the findings of this study are available from the corresponding author on reasonable request.

### Animals and Ethics Statement

All animal studies were conducted in accordance with regulations of the Institutional Animal Care and Use Committee at Northwestern University. All mice were housed in a conventional facility at Northwestern University under a 12-hour light cycle. Standard irradiated chow and autoclaved water were provided ad libitum. Euthanasia was performed by bilateral thoracotomy and sternotomy for terminal sample collection following induction of adequate general anesthesia.

### Antibiotic Treatment

C57BL/6J mice obtained from Jackson Laboratories (Bar Harbor, ME) underwent bedding mixing for 2 weeks, followed by treatment via the drinking water with vancomycin (0.5 mg/mL), sodium butyrate (100 mmol/L), vancomycin+butyrate, or sodium-matched control drinking water, as previously described.<sup>13</sup> Mice were randomized to treatment groups. Bedding mixing was performed to equilibrate animal housing conditions. After 5 weeks of drinking

water treatment, all animals underwent left femoral artery wire injury. The right side served as the uninjured control. Stool samples were collected before the start of water treatment, before carotid angioplasty, and on the day of euthanasia. Stool pellets were frozen in liquid nitrogen and stored at  $-80^{\circ}\text{C}$  until time of use.

### FFAR2 and FFAR3 Knockout Mice

Generation of FFAR2 and FFAR3 knockout mice has been previously reported.<sup>17,18</sup> Heterozygous FFAR2 and FFAR3 mice on a C57BL/6J background were kindly provided by Dr Brian T. Layden (University of Illinois at Chicago) and crossed to produce wild-type (WT) and knockout mice, which were genotyped as previously described.<sup>18</sup>

### Unilateral Femoral Artery Wire Injury

This mouse model of neointimal hyperplasia has been previously described.<sup>19</sup> In brief, mice were anesthetized with a single IP injection of a cocktail of ketamine (80 mg/kg) and xylazine (5 mg/kg). A 1.5-cm groin incision was made directly over the left femoral artery. The right femoral artery served as the unoperated control. The common femoral artery was dissected out along its length, including the side branches. Vascular control was obtained proximally and distally with noncrushing vascular clamps. An arteriotomy was made in a medial muscular arterial branch. A 0.014-inch guide wire was inserted through the arteriotomy into the common femoral artery, passed in and out 3 times, and then held in place for 5 minutes. Following injury, the guide wire was removed and the branch was ligated proximal and distal to the arteriotomy. The vascular clamps were removed, and restoration of flow to the common femoral artery was verified. The skin incision was closed with skin clips. At designated time points after surgery, the animals were anesthetized with isoflurane for terminal blood and tissue collection. Whole blood was collected by cardiac puncture. Serum was prepared and stored at  $-80^{\circ}\text{C}$  until use. Both femoral arteries are removed after in situ perfusion-fixation with paraformaldehyde.

### In Situ Evans Blue Dye Staining

Reendothelialization of the injured artery was assessed by staining with Evans blue dye (Sigma Aldrich, St Louis, MO). Following induction of adequate general anesthesia and creation of a midline laparotomy, 50  $\mu\text{L}$  of 5% Evans blue dye was injected into the abdominal aorta and allowed to circulate before flushing with 1 mL PBS. Both femoral arteries distal to the level of injury were transected. The injured segment of the left femoral artery and the corresponding segment of the right femoral artery were

removed, opened longitudinally, and photographed ex vivo adjacent to a ruler. The blue and total area of injury were calculated using ImageJ/FIJI software (National Institutes of Health, Bethesda, MD) after calibration with the ruler. The ratio of blue-stained area/the total area was calculated.

### Tissue Processing and Morphometric Analysis

Explanted arteries were fixed, embedded in optimal cutting temperature compound, sectioned, and stained, as previously described.<sup>20</sup> Digital images of hematoxylin-eosin-stained sections were obtained using a Leica DM2000 light microscope with a 20 $\times$  objective and camera. Morphometric analysis by investigators blinded to the experimental group was performed by using lumen, intima, and media areas and circumference that were measured or calculated using ImageJ/FIJI software after calibration. Sections were sampled at 35- $\mu\text{m}$  intervals along the length of the injured artery ( $\approx 2.5$  mm in length).

### Microbial DNA Preparation

Stool pellets were collected and stored at  $-80^{\circ}\text{C}$  before processing. Microbial DNA was extracted with the DNeasy PowerSoil DNA Isolation Kit (Qiagen, Hilden, Germany) following the manufacturer's protocol.

### 16S Ribosomal RNA-Based Analysis of Gut Microbial Composition and Diversity

Sequencing, assembly, taxonomic assignment, and diversity assessments were performed, as previously described.<sup>13</sup>

### Stool and Serum Butyrate Quantification

Samples were prepared, as previously described.<sup>21</sup> In brief, SCFAs in samples and standards were extracted in 50% acetonitrile, vortexed, and clarified by centrifugation. Supernatant (40  $\mu\text{L}$ ) was used for derivatization using 20  $\mu\text{L}$  200 mmol/L 3-nitrophenylhydrazine in 50% aqueous acetonitrile and 20  $\mu\text{L}$  120 mmol/L *N*-(3-dimethylaminopropyl)-*N'*-ethylcarbodiimide–6% pyridine. The solution then was diluted to 2 mL with 10% aqueous acetonitrile. Derivatized sample (50  $\mu\text{L}$ ) was mixed with 50  $\mu\text{L}$  of the internal standards, and 10  $\mu\text{L}$  of the resulting solution was used for liquid chromatography/mass spectrometry. Acetate, propionate, and butyrate, purchased from Sigma-Aldrich, were reacted with 3-nitrophenylhydrazine hydrochloride, which was custom synthesized by IsoSciences Inc (King of Prussia, PA), and *N*-(3-dimethylaminopropyl)-*N'*-ethylcarbodiimide at the same condition as the

samples and served as the internal standards. Liquid chromatography/mass spectrometry analysis was performed on a Sciex Qtrap 6500 mass spectrometry system (SCIEX, Framingham, MA) coupled to an Agilent 1290 ultraperformance liquid chromatography system (Agilent Technologies, Santa Clara, CA) using a Phenomenex high-performance liquid chromatography C18 column, 100 Å, 2.6 µm, and operating in multiple reaction mode. A gradient of buffer A (0.1% formic acid in water) and buffer B (0.1% formic acid in acetonitrile) was applied as follows: 0 minutes, 15% of buffer B; increase buffer B to 45% in 4 minutes; 45% to 100% in 0.2 minutes; kept B at 100% for 1.8 minutes. The column was equilibrated for 2 minutes at 15% B between the injections. Flow rate was 500 µL/min. The column temperature was 40°C, and the autosampler was kept at 4°C. Precursor (Q1) and product ion (Q3) m/z transitions were 194.1 → 137.1 for acetate, 200.1 → 143.1 for <sup>13</sup>C<sub>6</sub>-acetate, 208.1 → 165.1 for propionate, 214.1 → 143.1 for <sup>13</sup>C<sub>6</sub>-propionate, 222.1 → 137.1 for butyrate, and 228.1 → 143.1 for <sup>13</sup>C<sub>6</sub>-butyrate. The analytes and internal standards eluted at 6 minutes. Acetate and <sup>13</sup>C<sub>6</sub>-acetate peaked at 1.5 minutes, propionate and <sup>13</sup>C<sub>6</sub>-propionate peaked at 1.9 minutes, and butyrate and <sup>13</sup>C<sub>6</sub>-butyrate peaked at 2.6 minutes. All the samples were analyzed in triplicate.

### Quantitative Real-Time Polymerase Chain Reaction

Total RNA was extracted from mouse arteries using the RNeasy kit (Qiagen), and cDNA was generated using the QuantiTect Reverse Transcription Kit (Qiagen). Gene expression was assessed by quantitative real-time polymerase chain reaction using gene-specific primers of FFAR3 and housekeeping genes obtained from Qiagen: FFAR3 (QuantiTect primer assay QT01299144), β-actin (QT00095242), and GAPDH (QT00199633). Relative gene expression of FFAR3 was compared with the geometric mean of β-actin and GAPDH, as previously described.<sup>22</sup>

### Cell Culture and Scratch Assays

Primary cultures of human umbilical vein endothelial cells (ECs) at low passage were kindly provided by Dr William Muller (Northwestern University) and cultured in EGM-2 Endothelial Cell Growth Medium-2 BulletKit (Lonza, Basel, Switzerland). Human aortic VSMCs were obtained from Lonza and cultured in vascular cell basal medium containing the VSMC growth kit (ATCC, Manassas, VA). Scratch assays were performed, as previously described.<sup>13</sup> Cells were washed once, and 1-methylcyclopropane carboxylate (1-MCPC) (Sigma) (50–150 µmol/L) was added to starvation media containing 0% serum. The scratch was photographed at

24 and 48 hours. Treatment groups were performed in triplicate in each experiment. Closure of the scratch was quantified by area (for human umbilical vein ECs) or by cell number (for human aortic VSMCs) using ImageJ/FIJI. All experiments were conducted at least 3 times.

### Statistical Analysis

Statistical analysis was performed using Prism (GraphPad Software, San Diego, CA). Summary data are expressed for each group as mean±SEM. For comparison between 2 groups, an unpaired Student *t* test or Mann-Whitney *U* test was used, depending on the distribution of these data. *P*<0.05 was considered significant.

## RESULTS

### Depletion of Microbiota by Oral Vancomycin Exacerbates Neointimal Hyperplasia After Arterial Injury

Femoral artery wire injury was performed in C57BL/6 males (16–18 weeks old) after treatment with oral vancomycin. Vancomycin-treated mice had significantly more neointimal hyperplasia development 2 weeks after femoral artery wire injury compared with control-treated mice (Figure 1A and 1B), which correlated with significantly lower stool and serum concentrations of major SCFA butyrate, acetate, and propionate (Figure 1C). However, exogenous butyrate replacement in the vancomycin+butyrate-treated group partially mitigated the effect of vancomycin (Figure 1A and 1B). As shown in Figure 1B, neither vancomycin nor vancomycin+butyrate treatment affected the histological features of uninjured (right-sided) femoral arteries. As expected, vancomycin treatment also correlated with significant divergence in β diversity of fecal microbial samples from control samples (Figure 1C). Collectively, these data suggest an inverse correlation between microbe-derived butyrate and neointimal hyperplasia susceptibility after arterial injury.

### Effect of FFAR2 and FFAR3 on Neointimal Hyperplasia

FFAR2 and FFAR3 are both GPCRs for butyrate. We observed no gross differences in uninjured FFAR2 and FFAR3 WT and knockout femoral arteries by histological analysis (hematoxylin and eosin, Masson trichrome, or elastin staining) (Figure 2A, 2B, and 2C). Femoral artery wire injury was performed in age- and sex-matched FFAR2 and FFAR3 WT and knockout mice (16–18 weeks old) to clarify the role of these receptors to the arterial remodeling response to injury.



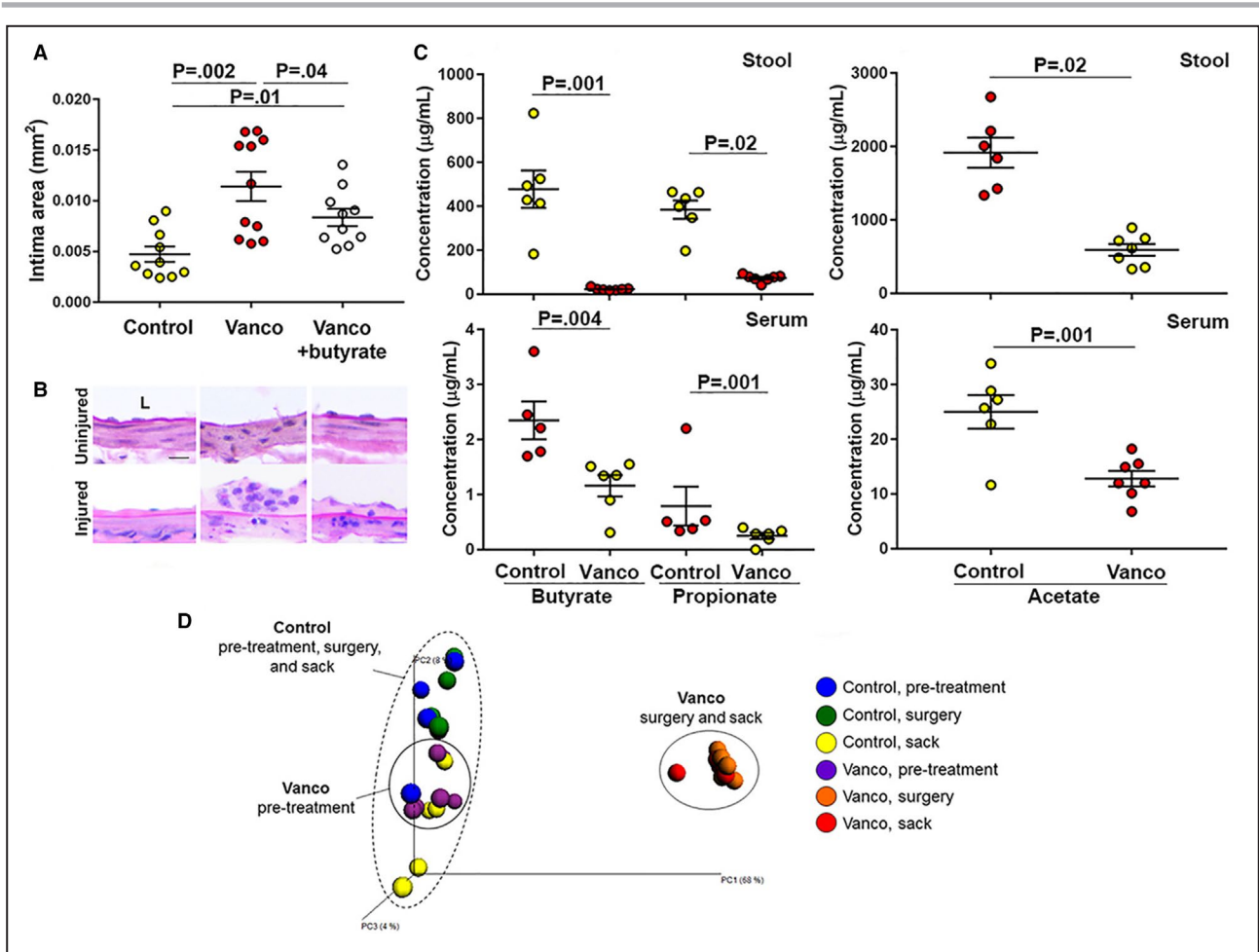


**Figure 1. Microbe-derived butyrate is implicated in susceptibility to neointimal hyperplasia after arterial injury.** **A**, Femoral artery wire injury was performed in C57BL/6 mice after 5 weeks of treatment with either oral vancomycin (vanco) or vanco+butyrate. Mice were euthanized 2 weeks after surgery, and neointimal hyperplasia was assessed in explanted arteries (N=10–12 per group). All P values represent comparisons between 2 groups (control vs Vanco, P=0.002; control vs Vanco+butyrate, P=0.01; Vanco vs Vanco+butyrate, P=0.04). **B**, Representative cross-sections of injured and uninjured femoral arteries in each treatment group are shown. Bar=25 μm. Lumen orientation of each arterial section is indicated by "L." **C**, Stool and serum concentrations of major short-chain fatty acids (SCFAs), butyrate, propionate, and acetate, were measured at the time of euthanasia. SCFA concentrations in the control and Vanco cohorts are shown (N=10–12 per group). **D**, Microbial shifts in the control and Vanco cohorts. Principal coordinate analysis of unweighted unique fraction metric (UniFrac) β diversity of microbiome samples in both groups at the time of surgery is shown (N=5 per group). Lines on each scatterplot (A and C) represent mean±SEM. Statistical analyses were performed with the Mann-Whitney U test (A and B).

There was a 1.4-fold increase in neointimal hyperplasia development in FFAR3 knockout mice compared with WT littermates (neointima area, WT versus knockout, 0.015±0.001 versus 0.022±0.002 mm<sup>2</sup>; P=0.01), but no difference between FFAR2 knockout mice and WT littermates (neointima area, WT versus knockout, 0.017±0.001 versus 0.013±0.001 mm<sup>2</sup>; P=not significant). Complete morphometric data, including media area, neointima/(neointima+media) and neointima/media, are shown in the Table. There were no instances of postoperative death or arterial thrombosis. Representative images of arterial cross-sections from injured and uninjured WT and knockout arteries are shown in Figure 2D, and scatterplots

of neointima area are shown in Figure 2E. FFAR3 knockout mice also had delayed reendothelialization compared with WT mice, as assessed by in situ Evans blue dye staining of injured arteries 5 days after arterial injury (Figure 3A and 3B). These data suggest a role for FFAR3, but not FFAR2, in modulating neointimal hyperplasia development after arterial injury, potentially by regulation of endothelial recovery.

### Expression of FFAR3 in Murine Peripheral Arteries

We next assessed the distribution of FFAR3 gene expression in peripheral arteries using quantitative

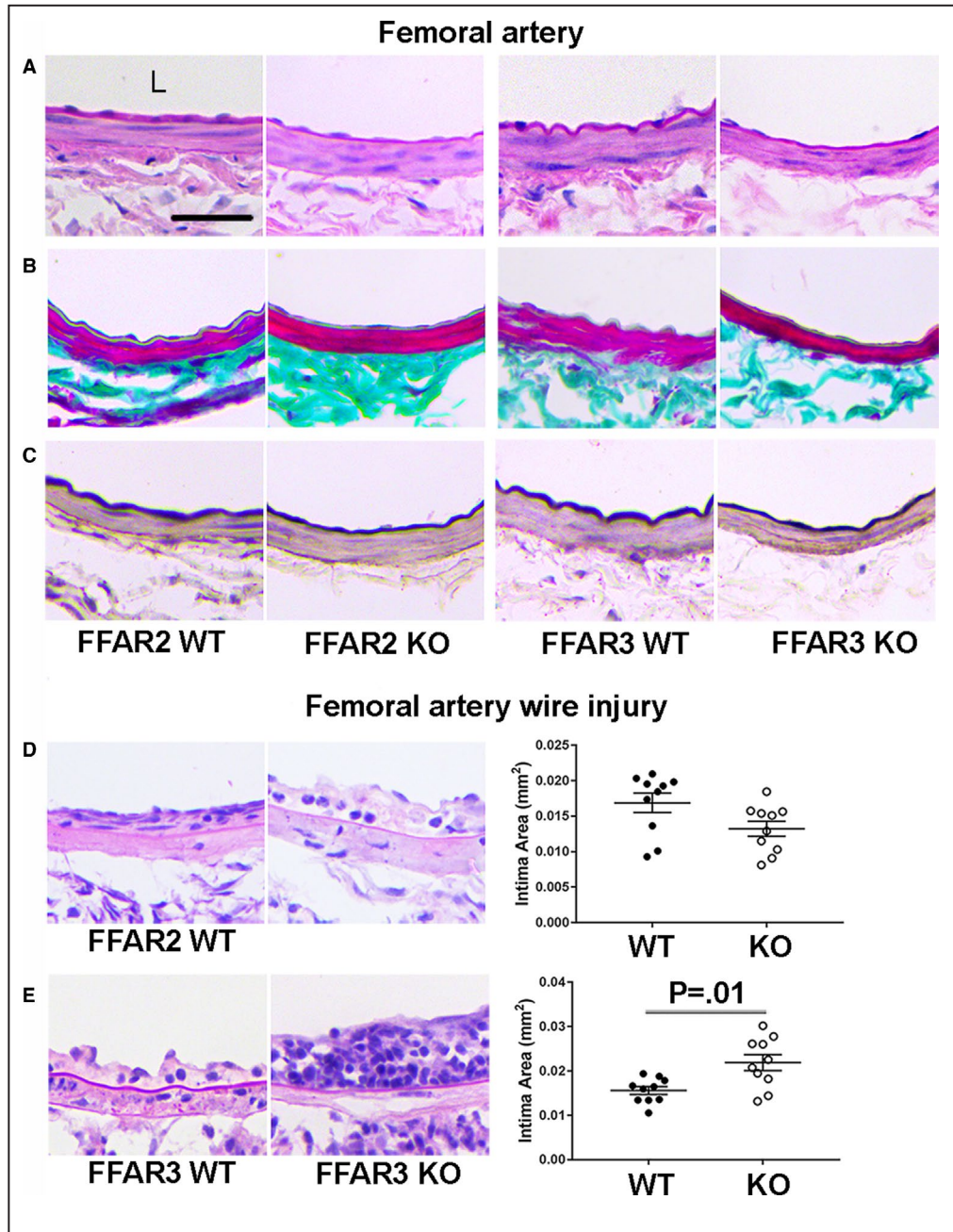


**Figure 2.** FFAR3 (Free fatty acid receptor 3), but not FFAR2 (free fatty acid receptor 2), modulates neointimal hyperplasia development after arterial injury.

Representative arterial sections of femoral arteries from FFAR2 and FFAR3 wild-type (WT) and knockout (KO) mice were analyzed histologically using hematoxylin-eosin (A), Masson trichrome (B), and elastin (C) staining. Bar=50 μm. Lumen orientation of each arterial section is indicated by "L." Femoral artery wire injury was performed in FFAR2 and FFAR3 KO mice and their respective WT littermates. Mice were euthanized 2 weeks after surgery, and neointimal hyperplasia was assessed in explanted arteries (N=10–12 per group). **D**, Representative photomicrographs of arterial sections from injured FFAR2 WT and KO arteries are shown (left panel). There was no significant difference in neointimal hyperplasia (P=0.91) between FFAR2 WT and KO mice (right panel) (N=10–12 per group). **E**, Representative photomicrographs of arterial sections from injured FFAR3 WT and KO arteries are shown (left panel). There was a significant increase in neointimal hyperplasia in FFAR3 KO compared with WT mice (right panel) (N=10–12 per group). Magnification and lumen orientation of arterial sections in D and E are the same as in A through C. Lines on each scatterplot represent mean±SEM, and statistical analyses were performed with the Mann-Whitney U test (D and E).

**Table. Morphometric Parameters of FFAR2 and FFAR3 WT and Knockout Femoral Arteries 2 Weeks After Wire Injury**

Parameter	FFAR2		P Value	FFAR3		P Value
	WT	Knockout		WT	Knockout	
Neointima, mm <sup>2</sup>	0.017±0.001	0.013±0.001	0.91	0.015±0.001	0.022±0.002	0.01*
Media, mm <sup>2</sup>	0.0134±0.0006	0.0147±0.002	0.53	0.0155±0.0004	0.0136±0.0004	0.007*
Neointima/(neointima+media)	0.375±0.016	0.439±0.034	0.07	0.418±0.016	0.526±0.019	0.001*
Neointima/media	0.756±0.062	0.775±0.263	0.13	0.709±0.036	1.518±0.177	0.007*

Values presented are mean±SEM. FFAR2 indicates free fatty acid receptor 2; FFAR3, free fatty acid receptor 3; and WT, wild type. \*P<0.05.

real-time polymerase chain reaction. FFAR3 mRNA was detected at varying levels in uninjured WT carotid artery, aorta, and femoral artery

(Figure 4A). In the femoral artery, FFAR3 mRNA increased 3-fold by 3 days after injury, as shown in Figure 4B.

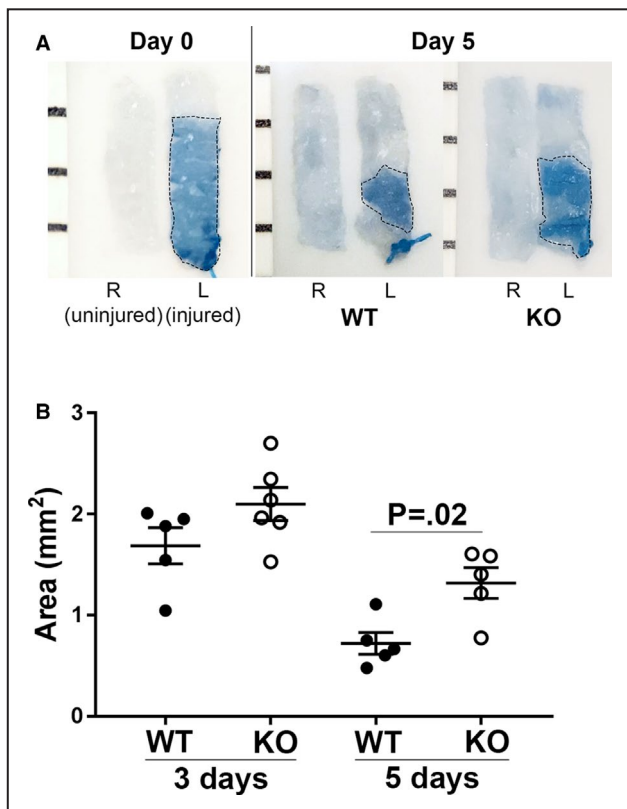


**Figure 3. FFAR3 (Free fatty acid receptor 3) modulates endothelial recovery after arterial injury.**

FFAR3 wild-type (WT) and knockout (KO) mice underwent femoral artery wire injury. At 3 or 5 days after injury, in situ Evans blue staining was performed. Arteries were explanted, opened longitudinally, and photographed adjacent to a ruler. **A**, Representative arteries explanted from an uninjured and injured femoral artery at day 0 (left panel) and at 5 days (right panel), showing increased recovery of the endothelium (ie, lack of blue staining) in the WT compared with the KO artery. Dotted lines indicate area of blue staining. **B**, Blue staining was quantified in each artery at 3 and 5 days. There was no significant difference in staining between WT and KO mice at 3 days (P=0.18). Lines on each scatterplot represent mean±SEM. N=5 to 6 per group per time point. Statistical analysis was performed with the Mann-Whitney U test (**B**). L indicates left; and R, right.

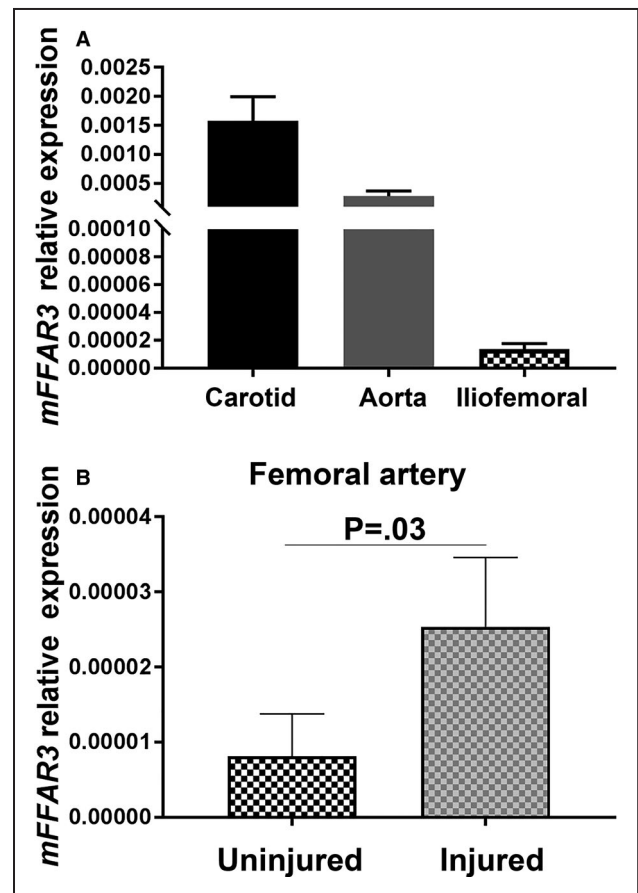


**Figure 4. Ffar3 gene expression in murine peripheral arteries.**

**A**, Total RNA was isolated from the indicated peripheral arteries of adult C57BL/6 mice, and cDNA was reverse transcribed, as described in the Methods section. *Ffar3* mRNA was quantified by quantitative polymerase chain reaction and gene expression was normalized to the geometric mean of *Actb* and *Gapdh* housekeeping genes and expressed as *Ffar3* relative expression. **B**, Relative expression of *Ffar3* in uninjured and injured femoral arteries. Arteries were harvested 3 days after injury. Four arteries were pooled together in each RNA sample and hence each bar represents 12 to 16 pooled arteries. Statistical analysis was performed with the Mann-Whitney U test (**B**).

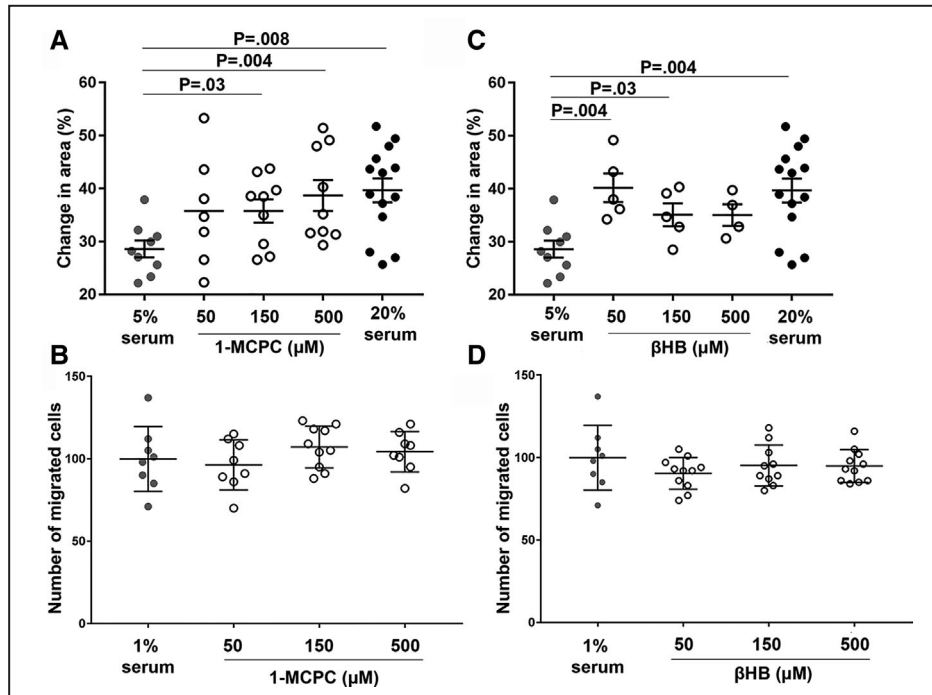


**Figure 5.** Pharmacologic activation of FFAR3 (free fatty acid receptor 3) in human umbilical vein endothelial cells (HUVECs) and human aortic vascular smooth muscle cells (HAoSMCs). HUVECs and HAoSMCs were plated in 12-well dishes and subjected to scratch assays after reaching subconfluence. Cells were treated with pharmacologic FFAR3 agonist 1-methylcyclopropane carboxylate (1-MCPC) or vehicle control. The scratch was photographed at the time of the scratch and 24 hours later. Closure of the scratch by proliferating and migrating cells was quantified by measuring area of the scratch (HUVECs) or counting number of migrated cells (HAoSMCs). **A**, Change in scratch area of HUVECs treated with 1-MCPC, expressed as percentage of original scratch area in each treatment group. The 20% serum represents the positive control. **B**, Number of cells filling the scratched area of HAoSMCs treated with 1-MCPC. There is no significant change between the 50-, 150-, and 500- $\mu\text{M}$  1-MCPC groups and 1% serum ( $P=0.91$ ,  $P=0.28$ , and  $P=0.46$ , respectively). Each circle represents a biological replicate. Lines represent means for the group  $\pm$  SEM. Statistical analysis was performed with the Mann-Whitney U test.

### Effect of Pharmacologic FFAR3 Agonists of EC and VSMC Migration and Proliferation

1-MCPC is a known pharmacologic agonist of FFAR3. Because FFAR3 appears to both modulate in vivo recovery of the endothelial layer after femoral artery wire injury and be expressed in the arterial wall, we next examined the effect of FFAR3 agonism in vitro. Human umbilical vein ECs and human aortic VSMCs were subjected to in vitro scratch assays with increasing doses of 1-MCPC or vehicle. Human umbilical vein ECs demonstrated augmentation in closure of the scratch area after treatment with 1-MCPC (Figure 5A). In contrast, 1-MCPC had no effect on human aortic VSMCs in the scratch assay (Figure 5B). These data suggest that activation of FFAR3 by the pharmacologic agonist 1-MCPC stimulates EC but not VSMC migration and proliferation, providing phenomenological evidence of cell-specific activity of FFAR3.

### DISCUSSION

The microbe-derived metabolite butyrate has been shown to have myriad physiological effects, including in the cardiovascular system, where it has a regulatory role in hypertension,<sup>23–26</sup> hypertrophic cardiomyopathy,<sup>27</sup> and atherogenesis.<sup>28</sup> Prior work by others has also demonstrated that butyrate has cell-specific effects on gene transcription because of its activity as a histone deacetylase inhibitor.<sup>29</sup> Butyrate and other major SCFAs, propionate and acetate, are also ligands of FFAR2 and FFAR3, which are GPCRs that couple the  $G_{\alpha}$  (FFAR2) and/or  $G_{i/o}$  (FFAR2 and FFAR3) pathways.<sup>15,30</sup> In this study, we demonstrate that antibiotic treatment alters gut microbial communities, depletes systemic SCFA concentration, and exacerbates neointimal hyperplasia development in a murine model of arterial injury, which is attenuated by exogenous butyrate dietary supplementation; that murine FFAR3 is present in multiple peripheral arteries; that FFAR3, but



not FFAR2, knockout mice have worsened neointimal hyperplasia development and delayed endothelial recovery after arterial injury compared with WT controls; and that pharmacologic FFAR3 agonists promote EC but not VSMC migration and proliferation. This study adds to our previous data suggesting a role for gut microbes in arterial remodeling after vascular surgery, and specifically provides a mechanistic link between microbe-derived butyrate, FFAR3, the endothelial response to injury, and neointimal hyperplasia.

This study corroborates our earlier study<sup>13</sup> in rats and work by many others that antibiotics significantly alter the gut microbial community and deplete butyrate. We specifically found that serum levels of butyrate were significantly depleted but still detectable after vancomycin treatment despite the steep concentration gradient<sup>31</sup> of SCFAs between the intestinal lumen and periphery. In humans, although there is an association between free fatty acids and atherosclerotic disease,<sup>32–38</sup> the association between free fatty acids and arterial restenosis after cardiovascular procedures is unknown. We used oral vancomycin as a tool to reduce gut biomass and thus the primary source of butyrate production. Although vancomycin has been shown to be toxic to ECs *in vitro*, this was demonstrated only with doses expected after intravenous infusions lasting 24 to 72 hours.<sup>39</sup> Because oral vancomycin is not absorbed systemically,<sup>40</sup> we would not anticipate any vancomycin-related change in FFAR3 expression or endothelial function. Moreover, we did not observe any histologic changes in uninjured mouse femoral arteries after oral vancomycin treatment (Figure 1B).

Existing data on the gene expression pattern of FFAR3 in the vasculature are also conflicting. A survey of tissues from adult C57BL/6 mice assessed transcript levels for 353 GPCRs and identified undetectable relative expression of FFAR3 in the aorta and low levels in the vena cava.<sup>41</sup> However, Pluznick et al<sup>42</sup> identified FFAR3 gene expression by real-time polymerase chain reaction in WT murine aorta, renal artery, and iliac artery, with relative expression highest in the renal artery>iliac artery>aorta. Interestingly, Natarajan et al<sup>43</sup> further localized aortic FFAR3 gene expression to the endothelial layer, because expression was not detected after endothelial denudation. EC expression of FFAR3 was also reported by Li et al.<sup>44</sup> Like Pluznick et al,<sup>42</sup> we also found differential FFAR3 gene expression in peripheral arteries (carotid>aorta>iliofemoral). Because our injury model is in the femoral artery, we also assessed for change in gene expression 3 days after injury and noted a marked increase in gene expression corresponding to a time point when the endothelial layer is recovering. Like others,<sup>43</sup> we found that commercially available antibodies to FFAR3 did not provide specific staining and hence were not used to assess protein expression.

Although butyrate has been shown to have multiple effects in ECs, including regulation of vascular adhesion molecule expression,<sup>45–48</sup> decreased inflammasome activation,<sup>49</sup> reduced inflammatory cytokine release to inflammatory stimuli,<sup>47</sup> reduction of the oxidative stress response,<sup>50</sup> and modulation of cell proliferation and angiogenesis in a dose-specific manner,<sup>51–54</sup> and enhancement of the efficacy of induced pluripotent stem cell derivation from human adult or fetal fibroblasts,<sup>55</sup> the distinction between FFAR3-mediated effects and effects mediated by histone deacetylase inhibition is unclear. Thus, we used a pharmacologic agonist of FFAR3, 1-MCPC, to specifically investigate the effect of cell-specific effects of FFAR3. Furthermore, because re-endothelialization strategies halt VSMC proliferation<sup>56–59</sup> and decrease neointima formation, we examined the role of 1-MCPC on both ECs and VSMCs in culture. Our data that 1-MCPC stimulates EC but not VSMC migration and proliferation, in combination with our observation that FFAR3 knockout mice had delayed endothelial recovery *in vivo*, implicate a protective effect of FFAR3 activation in the arterial remodeling response after injury.

Previous studies of FFAR3 knockout mice have suggested a role for FFAR3 in inflammation,<sup>60</sup> asthma,<sup>61</sup> metabolic disorders,<sup>18,62–64</sup> diabetes mellitus,<sup>62,65</sup> immune function,<sup>66</sup> and sympathetic tone.<sup>22,67,68</sup> This is the first report linking FFAR3 to the arterial injury response, and opens the door for future exploration of FFAR3 agonists as therapeutics or adjuncts for the prevention of neointimal hyperplasia after cardiovascular procedures.

There are several limitations to this study. Because concomitant vancomycin+butyrate treatment ameliorated the effect of vancomycin alone on neointimal hyperplasia, it is possible that other microbe-derived SCFAs, including propionate and acetate, which are also ligands for FFAR2 and FFAR3, have similar or related effects. However, the mitigation of the vancomycin phenotype with concomitant butyrate supplementation justifies our current focus on butyrate rather than other SCFAs. Strategies to boost *in vivo* butyrate in FFAR3 WT and knockout mice are under active investigation and will help strengthen the link between butyrate, FFAR3, and restenosis without concern for a competing effect of vancomycin. Furthermore, although we used human instead of mouse ECs and VSMCs for *in vitro* studies because of the availability of the human cells, other investigators have observed significant differences in the responses of human and mouse monocytes to stimulation by FFAR2 and FFAR3 agonists.<sup>69</sup> This could be addressed by repeating the *in vitro* experiments using mouse-derived WT and knockout ECs and VSMCs or using species-specific FFAR3 knockdown strategies (eg, small interfering RNA) to test cell-specific effects of FFAR3 activation. These gene knockdown strategies and the use of other pharmacologic receptor agonists

and antagonists of FFAR3 will also strengthen the link and provide important insights into the signaling events mediating FFAR3 activation and EC migration and proliferation. Furthermore, our study does not address the molecular mechanism by which FFAR3 modulates EC migration and proliferation or the possibility that modulation of systemic inflammation by FFAR3, and not direct FFAR3-dependent effects on ECs at the local site of arterial injury, contributes to neointimal hyperplasia; both possibilities are areas currently under active investigation. Finally, although the larger study includes mice from both sexes, females will be analyzed and reported separately as there is known sexual dimorphism in both neointimal hyperplasia susceptibility<sup>70</sup> and the microbiome.<sup>71</sup>

In summary, the present study demonstrates that microbe-derived butyrate has a protective role in neointimal hyperplasia development after arterial injury, which may be mediated by promotion of EC migration and proliferation in an FFAR3-dependent manner. The results highlight the potentially important role of the microbe-host interaction in the arterial remodeling response after cardiovascular surgery.

## ARTICLE INFORMATION

Received February 12, 2020; accepted May 15, 2020.

### Affiliations

From the Department of Surgery, Feinberg School of Medicine, Northwestern University (M.N., E.B. Chen, L.X., K.S., Q.J., M.E., K.J.H.); Department of Medicine, University of Illinois at Chicago and Jesse Brown VA Medical Center (M.P., B.T.L.); and Section of Gastroenterology, Department of Medicine, University of Chicago (E.B. Chang), Chicago, IL; and Geisel School of Medicine at Dartmouth, Hanover, NH (F.D.).

### Sources of Funding

This work was supported by the National Heart, Lung, and Blood Institute (grants K08HL130601 to Dr Ho and T32HL094293 to Drs Chen and Nooromid); the National Institute of Diabetes and Digestive and Kidney Diseases (grants P30DK42086 and R01DK115221 to Dr Chang and R01DK104927 and R01DK111848 to Dr Layden); the National Center for Advancing Translational Sciences (grant UL1TR001422 to Drs Ho, Chen, and Nooromid); the Department of Veterans Affairs, Veterans Health Administration Office of Research and Development (grant 1I01BX003382 to Dr Layden); Abbott Fund (Fellowship to Drs Chen and Nooromid); American College of Surgeons (Mentored Clinical Scientist Research Career Development Award to Dr Ho); Society for Vascular Surgery (Mentored Clinical Scientist Research Career Development Award to Dr Ho); and Division of Vascular Surgery, Northwestern University Feinberg School of Medicine (Lanterman Vascular Surgery Student Award to K. Shapiro, F. Demas, and M. Eskandari). Advanced microscopy was performed in the Analytical bioNanoTechnology Core (ANTEC) Facility of the Simpson Querrey Institute at Northwestern University. ANTEC is currently supported by the Soft and Hybrid Nanotechnology Experimental Resource (NSFECES-1542205). The Simpson Querrey Institute, Northwestern University Office for Research, US Army Research Office, and US Army Medical Research and Materiel Command have also provided funding to develop this facility.

### Disclosures

None.

## REFERENCES

- Benjamin EJ, Virani SS, Callaway CW, Chamberlain AM, Chang AR, Cheng S, Chiuve SE, Cushman M, Dellinger FN, Deo R, et al. American Heart Association Council on Epidemiology and Prevention Statistics Committee and Stroke Statistics Subcommittee. Heart disease and stroke statistics-2018 update: a report from the American Heart Association. *Circulation*. 2018;137:e67–e492.
- Jeong HC, Ahn Y, Hong YJ, Kim JH, Jeong MH, Kim YJ, Chae SC, Cho MC; and Other Korea Acute Myocardial Infarction Registry Investigators. Statin therapy to reduce stent thrombosis in acute myocardial infarction patients with elevated high-sensitivity C-reactive protein. *Int J Cardiol*. 2013;167:1848–1853.
- Walter DH, Schachinger V, Elsner M, Mach S, Auch-Schwelk W, Zeiher AM. Effect of statin therapy on restenosis after coronary stent implantation. *Am J Cardiol*. 2000;85:962–968.
- Kleemann A, Eckert S, von Eckardstein A, Lepper W, Schernikau U, Gleichmann U, Hanrath P, Fleck E, Neiss A, Kerber S, et al. Effects of lovastatin on progression of non-dilated and dilated coronary segments and on restenosis in patients after PTCA: the cholesterol lowering atherosclerosis PTCA trial (CLAPT). *Eur Heart J*. 1999;20:1393–1406.
- Abbruzzese TA, Havens J, Belkin M, Donaldson MC, Whittemore AD, Liao JK, Conte MS. Statin therapy is associated with improved patency of autogenous infrainguinal bypass grafts. *J Vasc Surg*. 2004;39:1178–1185.
- Kozuma K, Hara K, Yamasaki M, Morino Y, Ayabe S, Kuroda Y, Tanabe K, Ikari Y, Tamura T. Effects of cilostazol on late lumen loss and repeat revascularization after Palmaz-Schatz coronary stent implantation. *Am Heart J*. 2001;141:124–130.
- Take S, Matsutani M, Ueda H, Hamaguchi H, Konishi H, Baba Y, Kawarata H, Sugiura T, Iwasaka T, Inada M. Effect of cilostazol in preventing restenosis after percutaneous transluminal coronary angioplasty. *Am J Cardiol*. 1997;79:1097–1099.
- Zeller T, Rastan A, Macharzina R, Tepe G, Kaspar M, Chavarria J, Beschoner U, Schwarzwald U, Schwarz T, Noory E. Drug-coated balloons vs. drug-eluting stents for treatment of long femoropopliteal lesions. *J Endovasc Ther*. 2014;21:359–368.
- Jongsma H, Bekken JA, de Vries JP, Verhagen HJ, Fiore B. Drug-eluting balloon angioplasty versus uncoated balloon angioplasty in patients with femoropopliteal arterial occlusive disease. *J Vasc Surg*. 2016;64:1503–1514.
- Tang WHW, Backhed F, Landmesser U, Hazen SL. Intestinal microbiota in cardiovascular health and disease: JACC State-of-the-Art Review. *J Am Coll Cardiol*. 2019;73:2089–2105.
- Karlsson FH, Fak F, Nookaew I, Tremaroli V, Fagerberg B, Petranovic D, Backhed F, Nielsen J. Symptomatic atherosclerosis is associated with an altered gut metagenome. *Nat Commun*. 2012;3:1245.
- Liu H, Chen X, Hu X, Niu H, Tian R, Wang H, Pang H, Jiang L, Qiu B, Chen X, et al. Alterations in the gut microbiome and metabolism with coronary artery disease severity. *Microbiome*. 2019;7:68.
- Ho KJ, Xiong L, Hubert NJ, Nadimpalli A, Wun K, Chang EB, Kibbe MR. Vancomycin treatment and butyrate supplementation modulate gut microbe composition and severity of neointimal hyperplasia after arterial injury. *Physiol Rep*. 2015;3:e12627.
- Cummings JH, Pomare EW, Branch WJ, Naylor CP, Macfarlane GT. Short chain fatty acids in human large intestine, portal, hepatic and venous blood. *Gut*. 1987;28:1221–1227.
- Brown AJ, Goldsworthy SM, Barnes AA, Eilert MM, Tcheang L, Daniels D, Muir AI, Wigglesworth MJ, Kinghorn I, Fraser NJ, et al. The Orphan G protein-coupled receptors GPR41 and GPR43 are activated by propionate and other short chain carboxylic acids. *J Biol Chem*. 2003;278:11312–11319.
- Remesy C, Demigne C., & Morand C. Metabolism of short-chain fatty acids in the liver. In: Ummings JHC, Rombeau JL, Sakata T, eds. *Physiological and Clinical Aspects of Short-Chain Fatty Acids*. Cambridge, UK: Cambridge University Press; 1995: 171–190.
- Maslowski KM, Vieira AT, Ng A, Kranich J, Sierro F, Yu D, Schilter HC, Rolph MS, Mackay F, Artis D, et al. Regulation of inflammatory responses by gut microbiota and chemoattractant receptor GPR43. *Nature*. 2009;461:1282–1286.
- Samuel BS, Shaito A, Motoike T, Rey FE, Backhed F, Manchester JK, Hammer RE, Williams SC, Crowley J, Yanagisawa M, et al. Effects of the gut microbiota on host adiposity are modulated by the short-chain fatty-acid binding G protein-coupled receptor, Gpr41. *Proc Natl Acad Sci U S A*. 2008;105:16767–16772.
- Sata M, Maejima Y, Adachi F, Fukino K, Saiura A, Sugiura S, Aoyagi T, Imai Y, Kurihara H, Kimura K, et al. A mouse model of vascular injury

- that induces rapid onset of medial cell apoptosis followed by reproductive neointimal hyperplasia. *J Mol Cell Cardiol.* 2000;32:2097–2104.
20. Wun K, Theriault BR, Pierre JF, Chen EB, Leone VA, Harris KG, Xiong L, Jiang Q, Spedale M, Eskandari OM, et al. Microbiota control acute arterial inflammation and neointimal hyperplasia development after arterial injury. *PLoS ONE.* 2018;13:e0208426.
  21. Han J, Lin K, Sequeira C, Borchers CH. An isotope-labeled chemical derivatization method for the quantitation of short-chain fatty acids in human feces by liquid chromatography-tandem mass spectrometry. *Anal Chim Acta.* 2015;854:86–94.
  22. Colina C, Puhl HL 3rd, Ikeda SR. Selective tracking of FFAR3-expressing neurons supports receptor coupling to N-type calcium channels in mouse sympathetic neurons. *Sci Rep.* 2018;8:17379.
  23. Gomez-Arango LF, Barrett HL, McIntyre HD, Callaway LK, Morrison M, Dekker Nitert M, Group ST. Increased systolic and diastolic blood pressure is associated with altered gut microbiota composition and butyrate production in early pregnancy. *Hypertension.* 2016;68:974–981.
  24. Yang T, Rodriguez V, Malphurs WL, Schmidt JT, Ahmari N, Summers C, Martyniuk CJ, Zubcevic J. Butyrate regulates inflammatory cytokine expression without affecting oxidative respiration in primary astrocytes from spontaneously hypertensive rats. *Physiol Rep.* 2018;6:e13732.
  25. Yang T, Magee KL, Colon-Perez LM, Larkin R, Liao YS, Balazic E, Cowart JR, Arocha R, Redler T, Febo M, et al. Impaired butyrate absorption in the proximal colon, low serum butyrate and diminished central effects of butyrate on blood pressure in spontaneously hypertensive rats. *Acta Physiol.* 2019;226:e13256.
  26. Huat J, Leenders J, Taminiau B, Descy J, Saint-Remy A, Daube G, Krzesinski JM, Melin P, de Tullio P, Jouret F. Gut microbiota and fecal levels of short-chain fatty acids differ upon 24-hour blood pressure levels in men. *Hypertension.* 2019;74:1005–1013.
  27. Zhang L, Deng M, Lu A, Chen Y, Chen Y, Wu C, Tan Z, Boini KM, Yang T, Zhu Q, et al. Sodium butyrate attenuates angiotensin II-induced cardiac hypertrophy by inhibiting COX2/PGE2 pathway via a HDAC5/HDAC6-dependent mechanism. *J Cell Mol Med.* 2019;23:8139–8150.
  28. Kasahara K, Krautkramer KA, Org E, Romano KA, Kerby RL, Vivas EI, Mehrabian M, Denu JM, Backhed F, Lusk AJ, et al. Interactions between *Roseburia intestinalis* and diet modulate atherogenesis in a murine model. *Nat Microbiol.* 2018;3:1461–1471.
  29. Riggs MG, Whittaker RG, Neumann JR, Ingram VM. n-Butyrate causes histone modification in HeLa and Friend erythroleukaemia cells. *Nature.* 1977;268:462–464.
  30. Layden BT, Angueira AR, Brodsky M, Durai V, Lowe WL Jr. Short chain fatty acids and their receptors: new metabolic targets. *Transl Res.* 2013;161:131–140.
  31. Morrison DJ, Preston T. Formation of short chain fatty acids by the gut microbiota and their impact on human metabolism. *Gut Microbes.* 2016;7:189–200.
  32. Pirro M, Mauriege P, Tchernof A, Cantin B, Dagenais GR, Despres JP, Lamarche B. Plasma free fatty acid levels and the risk of ischemic heart disease in men: prospective results from the Quebec Cardiovascular Study. *Atherosclerosis.* 2002;160:377–384.
  33. Charles MA, Fontbonne A, Thibault N, Claude JR, Warnet JM, Rosselin G, Ducimetiere P, Eschwege E. High plasma nonesterified fatty acids are predictive of cancer mortality but not of coronary heart disease mortality: results from the Paris Prospective Study. *Am J Epidemiol.* 2001;153:292–298.
  34. Zhang HW, Zhao X, Guo YL, Zhu CG, Wu NQ, Sun J, Liu G, Dong Q, Li JJ. Free fatty acids and cardiovascular outcome: a Chinese cohort study on stable coronary artery disease. *Nutr Metab.* 2017;14:41.
  35. Breittling LP, Rothenbacher D, Grandi NC, Marz W, Brenner H. Prognostic usefulness of free fatty acids in patients with stable coronary heart disease. *Am J Cardiol.* 2011;108:508–513.
  36. Pilz S, Scharnagl H, Tiran B, Seelhorst U, Wellnitz B, Boehm BO, Schaefer JR, Marz W. Free fatty acids are independently associated with all-cause and cardiovascular mortality in subjects with coronary artery disease. *J Clin Endocrinol Metab.* 2006;91:2542–2547.
  37. Roy VK, Kumar A, Joshi P, Arora J, Ahanger AM. Plasma free fatty acid concentrations as a marker for acute myocardial infarction. *J Clin Diagn Res.* 2013;7:2432–2434.
  38. Miedema MD, Maziarz M, Biggs ML, Ziemann SJ, Kizer JR, Ix JH, Mozaffarian D, Tracy RP, Psaty BM, Siscovick DS, et al. Plasma-free fatty acids, fatty acid-binding protein 4, and mortality in older adults (from the Cardiovascular Health Study). *Am J Cardiol.* 2014;114:843–848.
  39. Drouet M, Chai F, Barthelemy C, Lebuffe G, Debaene B, Decaudin B, Odou P. Influence of vancomycin infusion methods on endothelial cell toxicity. *Antimicrob Agents Chemother.* 2015;59:930–934.
  40. Tedesco F, Markham R, Gurwith M, Christie D, Bartlett JG. Oral vancomycin for antibiotic-associated pseudomembranous colitis. *Lancet.* 1978;2:226–228.
  41. Regard JB, Sato IT, Coughlin SR. Anatomical profiling of G protein-coupled receptor expression. *Cell.* 2008;135:561–571.
  42. Pluznick JL, Protzko RJ, Gevorgyan H, Peterlin Z, Sipos A, Han J, Brunet I, Wan LX, Rey F, Wang T, et al. Olfactory receptor responding to gut microbiota-derived signals plays a role in renin secretion and blood pressure regulation. *Proc Natl Acad Sci U S A.* 2013;110:4410–4415.
  43. Natarajan N, Hori D, Flavahan S, Stepan J, Flavahan NA, Berkowitz DE, Pluznick JL. Microbial short chain fatty acid metabolites lower blood pressure via endothelial G protein-coupled receptor 41. *Physiol Genomics.* 2016;48:826–834.
  44. Li M, van Esch B, Henricks PAJ, Folkerts G, Garssen J. The anti-inflammatory effects of short chain fatty acids on lipopolysaccharide- or tumor necrosis factor alpha-stimulated endothelial cells via activation of GPR41/43 and inhibition of HDACs. *Front Pharmacol.* 2018;9:533.
  45. Miller SJ, Zaloga GP, Hoggatt AM, Labarrere C, Faulk WP. Short-chain fatty acids modulate gene expression for vascular endothelial cell adhesion molecules. *Nutrition.* 2005;21:740–748.
  46. Zapolska-Downar D, Siennicka A, Kaczmarczyk M, Kolodziej B, Naruszewicz M. Butyrate inhibits cytokine-induced VCAM-1 and ICAM-1 expression in cultured endothelial cells: the role of NF-kappaB and PPARalpha. *J Nutr Biochem.* 2004;15:220–228.
  47. Li M, van Esch B, Henricks PAJ, Garssen J, Folkerts G. Time and concentration dependent effects of short chain fatty acids on lipopolysaccharide- or tumor necrosis factor alpha-induced endothelial activation. *Front Pharmacol.* 2018;9:233.
  48. Ogawa H, Rafiee P, Fisher PJ, Johnson NA, Otterson MF, Binion DG. Butyrate modulates gene and protein expression in human intestinal endothelial cells. *Biochem Biophys Res Commun.* 2003;309:512–519.
  49. Yuan X, Wang L, Bhat OM, Lohner H, Li PL. Differential effects of short chain fatty acids on endothelial Nlrp3 inflammasome activation and neointima formation: antioxidant action of butyrate. *Redox Biol.* 2018;16:21–31.
  50. Aguilar EC, Santos LC, Leonel AJ, de Oliveira JS, ntosESa A, Navia-Pelaez JM, da Silva JF, Capettini LS, Mendes BP, Teixeira LG, et al. Oral butyrate reduces oxidative stress in atherosclerotic lesion sites by a mechanism involving NADPH oxidase down-regulation in endothelial cells. *J Nutr Biochem.* 2016;34:99–105.
  51. Ogawa H, Rafiee P, Fisher PJ, Johnson NA, Otterson MF, Binion DG. Sodium butyrate inhibits angiogenesis of human intestinal microvascular endothelial cells through COX-2 inhibition. *FEBS Lett.* 2003;554:88–94.
  52. Liu D, Andrade SP, Castro PR, Treacy J, Ashworth J, Slevin M. Low concentration of sodium butyrate from ultrabraid+NaBu suture, promotes angiogenesis and tissue remodeling in tendon-bones injury. *Sci Rep.* 2016;6:34649.
  53. Gururaj AE, Belakavadi M, Salimath BP. Antiangiogenic effects of butyric acid involve inhibition of VEGF/KDR gene expression and endothelial cell proliferation. *Mol Cell Biochem.* 2003;243:107–112.
  54. Tse CS, Williams DM. Inhibition of human endothelial cell proliferation in vitro in response to n-butyrate and propionate. *J Periodontol Res.* 1992;27:506–510.
  55. Mali P, Chou BK, Yen J, Ye Z, Zou J, Doney S, Brodsky RA, Ohm JE, Yu W, Baylin SB, et al. Butyrate greatly enhances derivation of human induced pluripotent stem cells by promoting epigenetic remodeling and the expression of pluripotency-associated genes. *Stem Cells.* 2010;28:713–720.
  56. Kim HJ, Kim JY, Lee SJ, Kim HJ, Oh CJ, Choi YK, Lee HJ, Do JY, Kim SY, Kwon TK, et al. alpha-Lipoic acid prevents neointimal hyperplasia via induction of p38 mitogen-activated protein kinase/Nur77-mediated apoptosis of vascular smooth muscle cells and accelerates postinjury reendothelialization. *Arterioscler Thromb Vasc Biol.* 2010;30:2164–2172.
  57. Kang DH, Lee DJ, Kim J, Lee JY, Kim HW, Kwon K, Taylor WR, Jo H, Kang SW. Vascular injury involves the overoxidation of peroxiredoxin type II and is recovered by the peroxiredoxin activity mimetic that induces reendothelialization. *Circulation.* 2013;128:834–844.
  58. Fuchs AT, Kuehl A, Pelisek J, Rolland PH, Mekkaoui C, Netz H, Nikol S. Inhibition of restenosis formation without compromising

- reendothelialization as a potential solution to thrombosis following angioplasty? *Endothelium*. 2008;15:85–92.
59. Breen DM, Chan KK, Dhaliwall JK, Ward MR, Al Koudsi N, Lam L, De Souza M, Ghanim H, Dandona P, Stewart DJ, et al. Insulin increases reendothelialization and inhibits cell migration and neointimal growth after arterial injury. *Arterioscler Thromb Vasc Biol*. 2009;29:1060–1066.
  60. Kim MH, Kang SG, Park JH, Yanagisawa M, Kim CH. Short-chain fatty acids activate GPR41 and GPR43 on intestinal epithelial cells to promote inflammatory responses in mice. *Gastroenterology*. 2013;145(396–406):e1–e10.
  61. Trompette A, Gollwitzer ES, Yadava K, Sichelstiel AK, Sprenger N, Ngom-Bru C, Blanchard C, Junt T, Nicod LP, Harris NL, et al. Gut microbiota metabolism of dietary fiber influences allergic airway disease and hematopoiesis. *Nat Med*. 2014;20:159–166.
  62. Tang C, Ahmed K, Gille A, Lu S, Grone HJ, Tunaru S, Offermanns S. Loss of FFA2 and FFA3 increases insulin secretion and improves glucose tolerance in type 2 diabetes. *Nat Med*. 2015;21:173–177.
  63. Bellahcene M, O'Dowd JF, Wargent ET, Zaibi MS, Hislop DC, Ngala RA, Smith DM, Cawthorne MA, Stocker CJ, Arch JR. Male mice that lack the G-protein-coupled receptor GPR41 have low energy expenditure and increased body fat content. *Br J Nutr*. 2013;109:1755–1764.
  64. Lin HV, Frassetto A, Kowalik EJ Jr, Nawrocki AR, Lu MM, Kosinski JR, Hubert JA, Szeto D, Yao X, Forrest G, et al. Butyrate and propionate protect against diet-induced obesity and regulate gut hormones via free fatty acid receptor 3-independent mechanisms. *PLoS One*. 2012;7:e35240.
  65. Priyadarshini M, Layden BT. FFAR3 modulates insulin secretion and global gene expression in mouse islets. *Islets*. 2015;7:e1045182.
  66. Voltolini C, Battersby S, Etherington SL, Petraglia F, Norman JE, Jabbour HN. A novel antiinflammatory role for the short-chain fatty acids in human labor. *Endocrinology*. 2012;153:395–403.
  67. Inoue D, Kimura I, Wakabayashi M, Tsumoto H, Ozawa K, Hara T, Takei Y, Hirasawa A, Ishihama Y, Tsujimoto G. Short-chain fatty acid receptor GPR41-mediated activation of sympathetic neurons involves synapsin 2b phosphorylation. *FEBS Lett*. 2012;586:1547–1554.
  68. Kimura I, Inoue D, Maeda T, Hara T, Ichimura A, Miyauchi S, Kobayashi M, Hirasawa A, Tsujimoto G. Short-chain fatty acids and ketones directly regulate sympathetic nervous system via G protein-coupled receptor 41 (GPR41). *Proc Natl Acad Sci U S A*. 2011;108:8030–8035.
  69. Ang Z, Er JZ, Tan NS, Lu J, Liou YC, Grosse J, Ding JL. Human and mouse monocytes display distinct signalling and cytokine profiles upon stimulation with FFAR2/FFAR3 short-chain fatty acid receptor agonists. *Sci Rep*. 2016;6:34145.
  70. Karas RH, Hodgkin JB, Kwoun M, Kregge JH, Aronovitz M, Mackey W, Gustafsson JA, Korach KS, Smithies O, Mendelsohn ME. Estrogen inhibits the vascular injury response in estrogen receptor beta-deficient female mice. *Proc Natl Acad Sci U S A*. 1999;96:15133–15136.
  71. Org E, Mehrabian M, Parks BW, Shipkova P, Liu X, Drake TA, Lusic AJ. Sex differences and hormonal effects on gut microbiota composition in mice. *Gut Microbes*. 2016;7:313–322.